Specific heat of superconducting films of indium and of indium alloyed with magnetic impurities *

B. C. Gibson,† D. M. Ginsberg, and P. C. L. Tai‡
Department of Physics and Materials Research Laboratory, University of Illinois at Urbana-Champaign, Urbana, Illinois 61801
(Received 12 September 1978)

We have measured the discontinuity in the specific heat Δc and the transition temperature T_c for superconducting quench-condensed films of indium, and of indium-manganese and indium-chromium alloys. These are the first measurements of Δc for a simple metal superconductor with magnetic 3-d transition-element impurities. It is useful to express the results in terms of Δc_0 and T_{c0}, the values for the pure superconductor. The Shiba theory indicates that $\Delta c/\Delta c_0$ is depressed more rapidly than T_c/T_{c0} as magnetic impurities are introduced into a superconductor. Our results confirm this prediction, but show an even greater depression than the Shiba theory predicts. Similar results have been obtained by previous workers for 3-d magnetic impurities in transition-metal superconductors. The present work also shows that Δc for pure indium increases with increasing disorder, where the degree of disorder is indicated by the residual resistivity of the sample. This result is to be expected qualitatively from Bergmann's studies of the transition temperature and energy gap width for disordered samples of indium. The present results, however, indicate that Δc increases roughly ten times more rapidly with the degree of disorder than would be estimated from his results.

I. INTRODUCTION

At the superconducting transition there is a discontinuity Δc in the electronic specific heat. During this investigation we have studied the depression of Δc caused by the introduction of magnetic impurities into the superconductor. We have determined, in particular, the effects of 3-d transition-element impurities, manganese and chromium, in a simple-metal superconductor, indium. We chose a simple metal for the host superconductor so that alloying with small amounts of the impurity would not greatly affect the density of states. We confined our studies to concentrations of the impurities which were low enough that impurity-impurity interactions were unimportant, i.e., low enough so that the transition temperature was not reduced below half that of the pure superconductor.[1]

The effects of magnetic impurities on superconductors have helped to provide insight into the fundamental nature of the superconducting phenomenon, and are instructive in understanding the interaction between the impurity atoms and the conduction electrons of metals. This investigation is one in a series of studies undertaken by this group, in which different techniques have been used to explore the properties of these systems. Reports have already appeared concerning thermal-conductivity measurements on In-Gd,[2] In-Mn,[3,4] In-Cr,[5] Pb-Gd,[2] and Pb-Mn,[4] and concerning upper critical-field measurements[6] on In-Mn and Pb-Mn.

II. THEORY

The interaction between a magnetic impurity atom and a conduction electron of the host metal is of the form

$$H_{ex} = -2J\vec{S}\cdot\vec{s}_e \tag{1}$$

if the orbital angular momentum of the impurity atom is quenched, where J is the exchange constant, $\vec{S}$ is the impurity spin, and $\vec{s}_e$ is the spin of the conduction electron. The interaction in Eq. (1) leads to the breaking of Cooper pairs, since the two elements of each pair are affected differently by the interaction.[7] This explains qualitatively the sharp depression in transition temperature and the rapid quenching of superconductivity that is observed for superconductors with magnetic impurities.[8-10]

The theory of this type of pair breaking was put on a quantitative footing by Abrikosov and Gor'kov (AG).[11] They developed a lowest-order perturbation treatment of the interaction between magnetic impurities and conduction electrons. The most spectacular prediction of the AG theory was gapless superconductivity.[7] The theory also predicted the dependence of the transition temperature T_c on the impurity concentration n:

$$\ln(T_c/T_{c0}) = \psi(\tfrac{1}{2}) - \psi(\tfrac{1}{2}+\rho), \tag{2}$$

where T_{c0} is the transition temperature of the pure superconductor, ψ is the digamma function,

$$\rho = \tfrac{1}{4}nN(0)J^2S(S+1)/k_BT_c, \tag{3}$$

k_B is Boltzmann's constant, and $N(0)$ is the density of states for one spin direction at the Fermi surface in the normal state. There is a critical concentration n_{cr} above which the superconductivity will not exist even at zero temperature. Equation (2) can be expressed in terms of n_{cr}:

$$\ln(T_c/T_{c0}) = \psi(\tfrac{1}{2}) - \psi(\tfrac{1}{2} + 0.1404 n T_{c0}/n_{cr} T_c). \quad (4)$$

Based on the AG theory, Skalski *et al.* derived a prediction for the discontinuity Δc in the electronic specific heat at the superconducting transition.[12] This is most conveniently expressed as a fraction of the same parameter for the pure superconductor, Δc_0:

$$\frac{\Delta c}{\Delta c_0} = \frac{\psi^2(\frac{1}{2})[1 - \rho\psi^1(\frac{1}{2}+\rho)]^2}{\psi^2(\frac{1}{2}+\rho) + \frac{1}{3}\rho\psi^3(\frac{1}{2}+\rho)} \frac{T_c}{T_{c0}}, \quad (5)$$

where $\psi^m(x)$ is the polygamma function, $d^m\psi(x)/dx^m$.

In general, the AG predictions usually describe well the behavior of superconducting systems in which the magnetic impurities are 4-*f* elements.[13] When the magnetic impurities are 3-*d* elements the AG theory is not so successful. This was shown in measurements of tunneling into In-Fe and Pb-Mn alloys,[14] of infrared absorption in Pb-Mn alloys,[15] and of thermal conductivity of In-Mn, Pb-Mn, and In-Cr alloys.[4,5]

A desirable extension of the theory is to treat the interaction to higher-order perturbation. Shiba[16] (and later, but independently, Rusinov[17]) did this, developing an exact theory for classical spins in superconductors. One fundamental difference between the Shiba theory and that of AG is that the new states produced in the energy gap by the magnetic impurities no longer arise necessarily just at the gap edge, but can arise within the gap, completely separated from the rest of the energy spectrum. These new states arise at an energy denoted as $\epsilon_0\Delta$, where Δ is the order parameter. ϵ_0 can be expressed in terms of the other parameters in the theory:

$$\epsilon_0 = \left| \frac{1 - [\frac{1}{2}\pi JSN(0)]^2}{1 + [\frac{1}{2}\pi JSN(0)]^2} \right|. \quad (6)$$

It turns out that Eq. (2) for the dependence of the transition temperature on the impurity concentration is also predicted by the Shiba theory, but with a new definition for ρ:

$$\rho = n(1 - \epsilon_0^2)/4\pi^2 N(0) k_B T_c. \quad (7)$$

Calculations[18] of Δc based on the Shiba theory give

$$\frac{\Delta c}{\Delta c_0} = \frac{\psi^2(\frac{1}{2})[1 - \rho\psi^1(\frac{1}{2}+\rho)]^2}{\psi^2(\frac{1}{2}+\rho) + \frac{1}{3}\rho(2\epsilon_0^2 - 1)\psi^3(\frac{1}{2}+\rho)} \frac{T_c}{T_{c0}}. \quad (8)$$

We will compare our results to this prediction. For the limiting case of weak interaction, $\epsilon_0 \to 1$, this and all the other predictions of the Shiba theory reduce to those of AG. For $\epsilon_0 \neq 1$, the Shiba theory predicts that $\Delta c/\Delta c_0$ will be reduced more rapidly relative to T_c/T_{c0} than in the AG case. The reduction is most rapid when $\epsilon_0 = 0$.

Müller-Hartmann and Zittartz (MHZ) have also extended the AG theory, in this case retaining the quantum-mechanical nature of the impurity spin.[19,20] Retention of the quantum-mechanical nature of the impurity spin is important; for example, it is required to explain the Kondo effect in normal metals. The MHZ theory was initially limited to the case of one impurity atom, although it has been used as the basis for approximate treatments, which led to the remarkable prediction of reentrant superconductivity.[21] Recently, Schuh and Müller-Hartmann have obtained a self-consistent extension of the MHZ theory which is applicable to finite impurity concentrations.[22] The results for Δc are difficult to calculate, and are dependent on two parameters, the Kondo temperature and the impurity spin. Since neither of these quantities are known for our alloys, we will confine ourselves to noting that, for some values of these parameters, $\Delta c/\Delta c_0$ is found to decrease more rapidly relative to T_c/T_{c0} than is predicted by Shiba, even for $\epsilon_0 = 0$.[20]

III. PREVIOUS WORK

The previous work on superconducting systems containing magnetic impurities has been reviewed in Refs. 13, 23, and 24. Of particular interest is Fig. 3 in Ref. 24, which illustrates the results obtained for $\Delta c/\Delta c_0$ for a number of alloys. The heat-capacity measurements which involve 3-*d* elements as the impurities are limited to Al-Mn,[25,26] Zn-Mn,[27] Zn-Cr,[28] and Mo-Fe.[29] In the only case where the host superconductor was a simple metal, Al-Mn, the results show that the impurity loses its magnetic character, so Δc scales directly with T_c. In the other three cases, however, the reduction in $\Delta c/\Delta c_0$ is so sharp when compared to T_c/T_{c0} that the data lie below even the most extreme prediction ($\epsilon_0 = 0$) of the Shiba theory.

The only previous measurements on the superconducting properties of In-Mn alloys have been done on the transition temperature,[30] thermal conductivity,[3,4] and upper critical field.[6] The recent thermal-conductivity measurements[4] indicate that In-Mn can be described well by the Shiba theory with $\epsilon_0 = 0.85$. The previous work on In-Cr has been confined to measurements of the transition temperature[30] and the thermal conductivity.[5] The thermal-conductivity measurements indicate that In-Cr is also well described by the Shiba theory with $\epsilon_0 = 0.70$.

IV. EXPERIMENTAL METHODS

A. General description

Our alloys were not stable at room temperature,[31] and so they were prepared as films, quench condensed on a substrate in the cryostat.[32] This was of an all-metal design with the evaporation boat located at the bottom. The substrate holder was made of copper, and was attached to a liquid-helium tank. It was surrounded by two heat shields, the inner one connected to a second liquid-helium tank and the outer to a liquid-nitrogen tank. The substrate was visible from the evaporation boat through holes in the heat shields, which were normally covered by shutters. The back of the substrate was cooled by a pool of liquid helium during the condensation of the sample film. The region in back of the substrate was then evacuated before the heat-capacity measurements were made.

Because the discontinuity in the heat capacity was only about 3% of the total heat capacity, we used ac calorimetry to determine the size of the discontinuity. During the data-taking process the substrate holder's temperature was maintained by an electronic temperature control, so it varied by less than 50 μK.[33]

B. Sample preparation

The preparation of the ingots of the sample material is described elsewhere.[4,5] The sample film was produced in the cryostat by individually evaporating approximately 60 pellets of the sample material from a tungsten boat, which was at a temperature of about 1500 °C. The temperature of the boat was measured by optical pyrometry, and was reproduced to within 50 °C from run to run. The sample film was 0.8 cm in diameter, and roughly 4000 Å thick.

Prior to the evaporation of the pellets, the substrate holder was cooled to below 1.5 K, and helium gas was leaked into the region behind the substrate. The helium gas condensed and formed a pool of superfluid helium behind the substrate. By this means the substrate was held at a temperature of about 2 K during the condensation of the sample film.

C. Substrate

The substrate was similar to that used by Zally and Mochel.[34] It was a piece of Pyrex (1.3 cm in diameter and approximately 3 μm thick) attached at its edges to a copper substrate holder. A schematic cross-section diagram of the substrate is shown in Fig. 1. A number of auxiliary films needed to be vacuum deposited on to the substrate before it was ready to be used in the experiment. A 5000-Å-thick layer of silver was deposited on the back side of the substrate to serve as an isotherm. The heater required for the heat-capacity measurements was a film of Chromel-A, approximately 90 Å thick. It was insulated electrically from the sample by a 5000-Å-thick layer of silicon monoxide. Electrical connections were made to the heater by 400-Å-thick gold leads. Four other gold leads were used to make resistance measurements of the sample film.

The sample thermometer was a piece of Ga-doped germanium about 1.0 mm on a side and 0.1 mm thick. The thermometer was attached to the back of the substrate by Torr seal.[35]

D. ac heat-capacity technique

To provide the required precision for the heat-capacity measurements, we used the ac calorimetry technique of Sullivan and Seidel.[36,37] We shall discuss the technique briefly and introduce some equations in order to show how it is especially useful for making accurate measurements of the size of a small sudden change in the sample's heat capacity.

A model of our calorimeter is shown schematically in Fig. 2. The sample has a heat capacity C_1, and is connected to a heat sink through a thermal link with a thermal conductance K_1. A thermometer with heat capacity C_2 is connected to the sample through a thermal link with thermal conductance K_2. The response of the calorimeter is determined from two time constants, an external time constant $\tau_1 = C_1/K_1$, which determines how quickly the system comes into equilibrium with the surrounding heat sink, and an internal time constant $\tau_2 = C_2/K_2$, which determines how quickly the thermometer comes into equilibrium with the sample. The case of interest here is where τ_1 is much

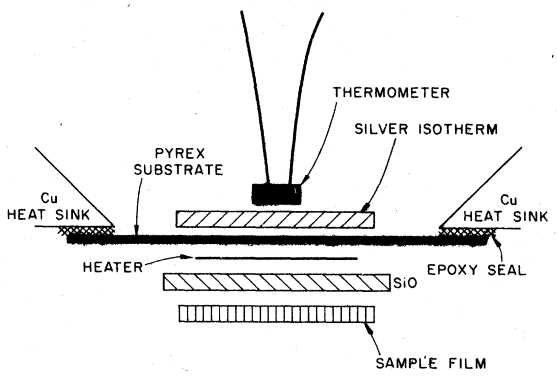

FIG. 1. Schematic cross-section diagram of the substrate with the sample film.

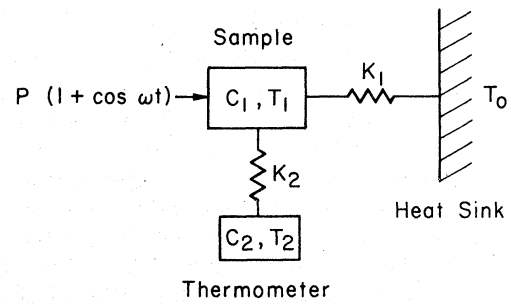

FIG. 2. Schematic model of the calorimeter used in this experiment. The symbols are defined in Sec. IV D.

greater than τ_2, so that

$$s \equiv \tau_2/\tau_1 \ll 1. \tag{9}$$

For our samples, s is typically 1/30.

An electric heater with resistance R_h is attached to the sample, and a voltage $V_0 \cos\frac{1}{2}\omega t$ is applied across the heater. The power dissipated is $P(1+\cos\omega t)$, where $P = V_0^2/2R_h$. The temperature of the thermometer is

$$T_2 = T_0 + T_{dc} + T_{ac}\cos(\omega t - \phi), \tag{10}$$

where T_0 is the temperature of the heat sink, $T_{dc} = P/K_1$ is the amount by which the average temperature of the thermometer is raised above that of the sink, T_{ac} is the amplitude of the sinusoidal temperature response to the sinusoidal heating, and ϕ is the corresponding phase shift. The quantity of interest is T_{ac}, since that is what we are able to measure:

$$T_{ac} = P/\omega(C_1^2 + C_1^2\omega^2\tau_2^2 + 2C_1C_2 + K_1^2\omega^{-2} + C_2^2 + K_1^2\tau_2^2 + 2C_2K_1\tau_2)^{1/2}. \tag{11}$$

We can rewrite this rather cumbersome expression as

$$T_{ac} = F(\omega)P/\omega[C_1(1+s) + C_2], \tag{12}$$

where $F(\omega)$ is the frequency response

$$F(\omega) = [1 + s\omega^{-2}\omega_0^2(1 - \omega^2\omega_0^{-2})^2(1 + s + C_2C_1^{-1})^{-2}]^{-1/2} \tag{13}$$

for which ω_0 is defined by

$$\omega_0 = (\tau_1\tau_2)^{-1/2}. \tag{14}$$

The phase shift can also be expressed in terms of $F(\omega)$:

$$\phi = \sin^{-1}F(\omega). \tag{15}$$

At ω_0, $F(\omega)$ is a maximum, with $F(\omega_0) = 1$, so that

$$T_{ac} = P/\omega[C_1(1+s) + C_2] \tag{16}$$

$$\simeq P/\omega C, \tag{17}$$

where C is the total heat capacity $C_1 + C_2$. So by knowing T_{ac}, P, and ω, one can determine

$$C' \equiv P/\omega T_{ac}, \tag{18}$$

where $C' \simeq C$.

Plotted against the logarithm of the frequency, $F(\omega)$ is a symmetric function centered at ω_0. At a given temperature, C_1 and C_2 are constant, so one can test the frequency response of the calorimeter by varying the applied frequency and measuring T_{ac}, P, and ω. According to Eq. (12), $\omega T_{ac}/P$ should be proportional to $F(\omega)$. The results of such a test on an actual calorimeter are shown in Fig. 3. Defined in Eq. (13), $F(\omega)$ is shown as a solid curve, with τ_1, τ_2, and the maximum response chosen to give the best fit to the data. As can be seen, the frequency response of the actual calorimeter agrees well with the predicted response of our model.

In the experiment, T_{ac}, P, and ω were measured to give the heat capacity according to the approximate equation (17). This leads to a systematic deviation of our results from the total heat capacity. The deviation is small (of order s, i.e., a few percent), and could be corrected for by our knowledge of the time constants. We do not apply such a correction, because it is unnecessary to do so when determining the size of a small change in the heat capacity (e.g., ΔC at the superconducting transition), as we shall now show.[32] We assume that the change in the heat capacity of the sample ΔC_1 is small compared to the total heat capacity $C_1 + C_2$. Using Eqs. (11) and (18), we can

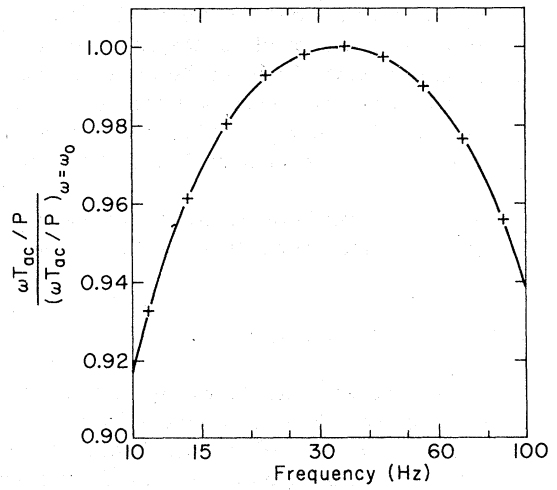

FIG. 3. Normalized frequency response $(\omega T_{ac}/P)/(\omega T_{ac}/P)_{\omega=\omega_0}$ of a calorimeter. The curve represents the predicted response $F(\omega)$ from Eq. (13). The maximum response $(\omega T_{ac}/P)_{\omega=\omega_0}$, the external time constant τ_1, and the internal time constant τ_2 were chosen to give the best fit to the data.

write C' as a function of C_1:

$$C' = (C_1^2 + C_1^2\omega^2\tau_2^2 + 2C_1C_2 + K_1^2\omega^{-2} + C_2^2 + K_1^2\tau_2^2 + 2C_2K_1\tau_2)^{1/2}. \quad (19)$$

If C_1 changes by an amount ΔC_1, then C' changes by an amount

$$\Delta C' = \Delta C_1 \frac{dC'}{dC_1} + \tfrac{1}{2}\Delta C_1^2 \frac{d^2C'}{dC_1^2} + \cdots . \quad (20)$$

Evaluating the derivatives of C' with respect to C_1, we obtain

$$\frac{dC'}{dC_1} = \frac{C_1 + C_1\omega^2\tau_2^2 + C_2}{C'} \quad (21)$$

and

$$\frac{d^2C'}{dC_1^2} = \frac{(1+\omega^2\tau_2^2)C'^2 - (C_1 + C_1\omega^2\tau_2^2 + C_2)^2}{C'^3}. \quad (22)$$

At $\omega = \omega_0$, we can simplify our expressions for C' and its derivatives:

$$C' = C_1 + sC_1 + C_2, \quad (23)$$

$$\frac{dC'}{dC_1} = 1, \quad (24)$$

and

$$\frac{d^2C'}{dC_1^2} = \frac{s}{C_1 + sC_1 + C_2} \simeq \frac{s}{C_1 + C_2}. \quad (25)$$

So, at ω_0, we find that

$$\Delta C' \simeq [1 + \tfrac{1}{2}s\Delta C_1(C_1 + C_2)^{-1}]\Delta C_1 . \quad (26)$$

In this experiment s was typically 1/30, and the change in the heat capacity at the superconducting transition was typically 3% of the total heat capacity, so at ω_0 the difference between $\Delta C'$ and ΔC_1 was less than 0.1% of ΔC_1, which was well below the uncertainty in the measured size of the discontinuity.

If the calorimeter is operated at a frequency near but not exactly equal to ω_0, we set $\omega = \omega_0(1+\delta)$. Then

$$\Delta C' \simeq [1 + 2\delta sC_1(C_1 + C_2)^{-1}]\Delta C_1. \quad (27)$$

Even in this case the difference between $\Delta C'$ and ΔC_1 is negligible ($<1\%$ of ΔC_1) near enough to ω_0 (within approximately 20% of ω_0). It was possible to set the operating frequency ω with great accuracy; the only difficulty was in determining accurately ω_0. We determined ω_0 for each run by making frequency-response measurements such as those shown in Fig. 3, and we estimate that the values we obtained were within 10% of the correct ones, so that $|\delta| \lesssim 0.1$.

E. Heat-capacity electronics

A block diagram of the electronics used in the heat-capacity measurement is given in Fig. 4. An oscillator provided power to the sample heater through an attenuator. This caused a sinusoidal variation in the temperature of the thermometer which was reflected in a sinusoidal variation in its resistance. A constant current was put through the sample thermometer, and so a sinusoidal voltage was developed across it. This voltage had an amplitude V_{ac} which could be directly related to T_{ac}:

$$T_{ac} = V_{ac}\frac{dT}{dR} I_T^{-1}, \quad (28)$$

where I_T is the current through the thermometer and dT/dR is the derivative of the temperature with respect to the resistance of the thermometer, determined by calibrating the thermometer. In this experiment the power applied to the sample was adjusted to give $T_{ac} = 2$ mK.

The null technique of Griffin and Mochel[38] was used to measure V_{ac}. The electrical signal from the thermometer was applied to one input of a preamplifier while a square wave of the same frequency and phase was applied to the other input. The amplified difference of these two signals was monitored by a lock-in amplifier, which served as a null detector. The amplitude of the square wave could be adjusted to null out the signal from the thermometer with four-digit precision, and the small off-null output signal provided by the lock-in was displayed on a chart recorder.

A similar arrangement was used to measure the voltage across and the current passing through the sample heater. The voltage across either the sample heater itself or a standard resistor in

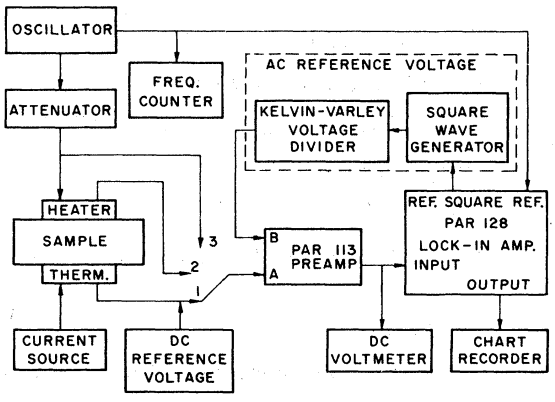

FIG. 4. Block diagram of the ac heat-capacity electronics.

series with it was simply applied to the "A" input of the preamplifier in place of the voltage from the sample thermometer.

The dc voltage across the thermometer was also measured by a null technique. A dc reference voltage was applied in series with the voltage across the thermometer, and this reference voltage was adjusted to null out the dc component of the voltage across it. The reference voltage was produced by passing an adjustable current through a 100-Ω resistor. This same current also passed through a 10-kΩ resistor, and the voltage across this larger resistor was directly measured to determine the reference voltage.

F. Film thickness

In order to convert the discontinuity in the heat capacity ΔC into a discontinuity in the specific heat Δc it was necessary to divide ΔC by the amount of sample material, which was determined from the film thickness. Four microscope cover slides were arranged around the hole in the sample mask to serve as dummy substrates. During the evaporation of the sample material the dummy substrates were partially covered by a second mask. After the run was over, the dummy substrates were removed from the cryostat, and were coated with a 1000-Å-thick layer of silver. At the edge where the mask had covered the dummy substrates there was a step in the height of the silver film. The height of the step was just the thickness of the underlying layer of sample material. The step height was measured by multiple-beam interferometry.[39] By this means we were able to measure the thickness of our films to an accuracy of about 1%.

G. Data analysis

We determined ΔC from the data as follows. Outside the transition region the heat capacity varied smoothly and could be described by two functions, $C_N(T)$ for the normal-state data and $C_S(T)$ for the superconducting-state data. We fitted polynomials in T to the data to obtain $C_S(T)$ and $C_N(T)$. No more than three parameters were used for each of these functions, and the fits showed good agreement with the data (the scatter of the data from the fitted functions was typically less than 0.02% of the total heat capacity). We determined ΔC and T_c by extrapolating $C_S(T)$ and $C_N(T)$ to the transition temperature, thereby essentially reproducing the behavior of an ideal superconductor with a zero-width transition. For ΔC we used the difference between the fitted heat capacities at the transition temperature, $C_S(T_c) - C_N(T_c)$. The transition temperature was assigned so that the area (entropy) under a curve of C/T vs T was preserved in going from the actual data to the idealized widthless transition.

V. RESULTS

Figures 5–8 show total heat capacity divided by temperature for our samples. The heat-capacity data are tabulated in Ref. 32. The contribution to the total heat capacity from the substrate, thermometer, etc., was not the same for each run, so some of the curves are displaced in order to show them together, using a reasonable scale. The slopes of some of the displaced curves are steeper than those of the undisplaced curves because they represent a larger heat capacity.

A summary of the results obtained on the sample films is given in Table I. The quantities of interest in comparing the data to the theoretical predictions are T_c/T_{c0} (the transition temperature normalized to that of the pure metal) and $\Delta c/\Delta c_0$

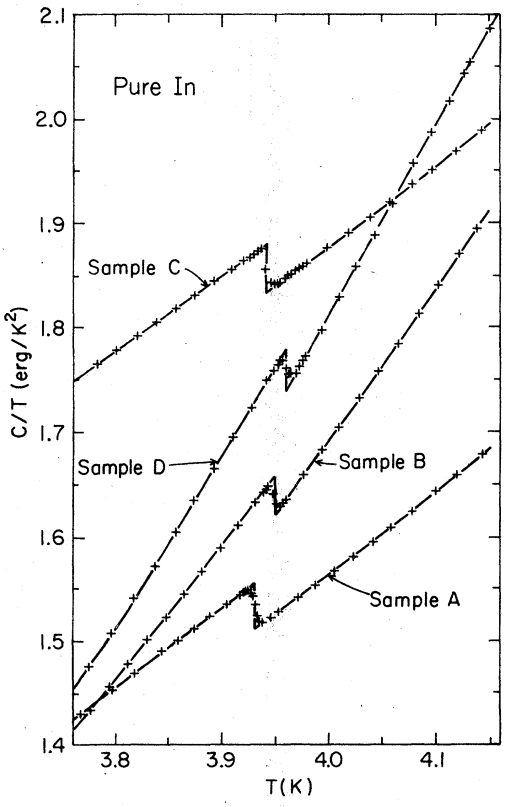

FIG. 5. Total heat capacity C divided by temperature T for runs A–D. The contribution to the total heat capacity from the substrate, thermometer, etc., was not the same for each run, so the data for runs B and D have been displaced downward by 2.8 erg/K² in order to show them with the data from the other two runs.

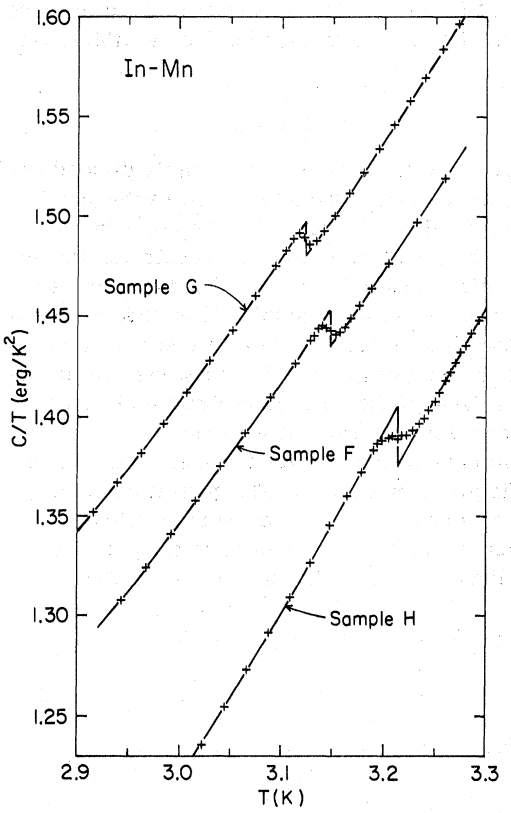

FIG. 6. Total heat capacity C divided by temperature T for runs F–H. The data for runs G and H have been displaced downward by 0.48 erg/K^2.

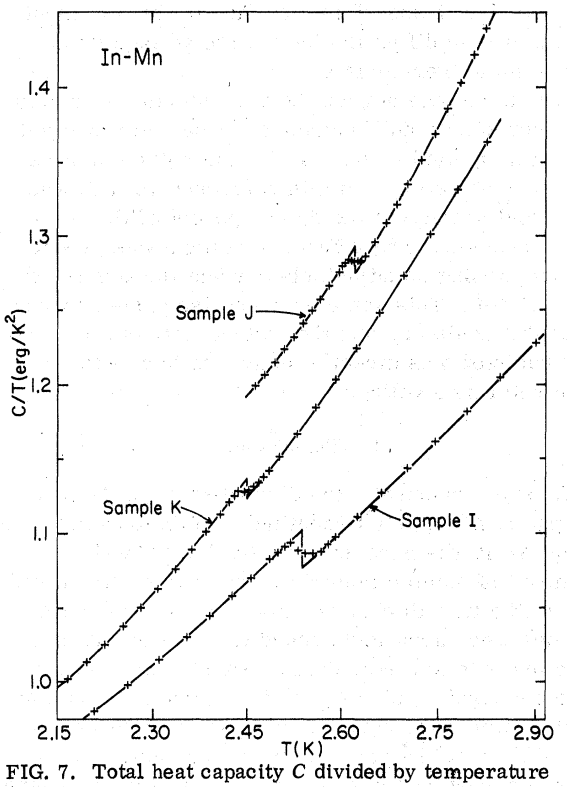

FIG. 7. Total heat capacity C divided by temperature T for runs I–K. The data for run I have been displaced upward by 0.3 erg/K^2. The data for run J have been displaced downward by 0.3 erg/K^2.

(the discontinuity in the specific heat normalized to that of the pure metal). We use the average values for the four runs of pure indium for T_{c0} and Δc_0. A graph of $\Delta c/\Delta c_0$ plotted against T_c/T_{c0} is given in Fig. 9 for the alloy samples.

The dependence of the transition temperature on impurity concentration is shown in Fig. 10, where the solid line is the AG prediction for an empirically fitted critical concentration of 760 at. ppm. The lower of the two points at $n/n_{cr} \simeq 0.4$ (run I) was not used in determining the critical concentration, because the transition temperature for that point seemed to be anomalously low.

VI. DISCUSSION

A. Pure indium

Data were obtained on four films of quench-condensed pure indium (99.999% pure). These measurements were made to provide a standard against which the alloy samples could be compared. For the transition temperature of the pure superconductor, T_{c0}, we obtained a value of 3.946 K, with an uncertainty of less than 0.2% in the de-

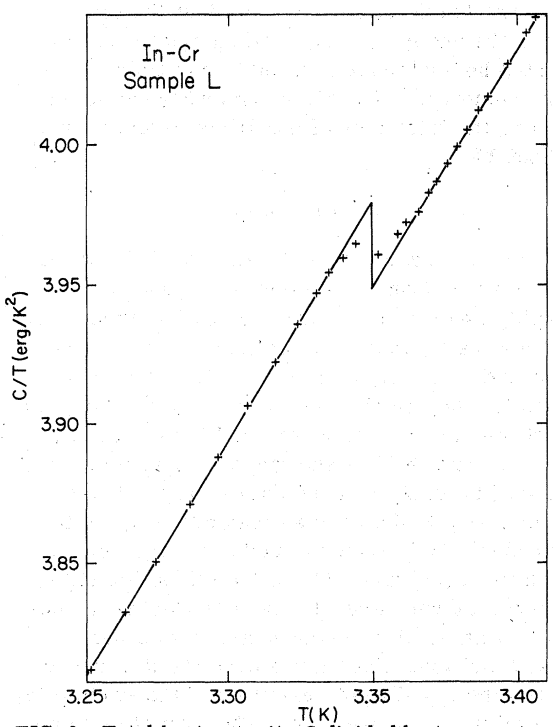

FIG. 8. Total heat capacity C divided by temperature T for run L.

TABLE I. Data summary. Impurity concentration n, film thickness D, electrical resistivity ρ, resistive transition temperature, 10%-90% resistive transition width, heat-capacity transition temperature, 10%-90% heat-capacity transition width, ratio of the heat-capacity transition temperature to that of the pure material, discontinuity in the heat capacity ΔC normalized by the film thickness, and ratio of the discontinuity in the specific heat to that of the pure material.

					Resistive		Heat capacity				
Run	Material	n (at. ppm)	D (Å)	ρ ($\mu\Omega$ cm)	T_c (K)	Width (mK)	T_c (K)	Width (mK)	T_c/T_{c0}	$\Delta C/D$ (μerg/K Å)	$\Delta c/\Delta c_0$
A	In	0	4060	3.65	4.136	193	3.931	9	0.996	42.03	1.191
B	In	0	5187	3.19	4.276	31	3.948	8	1.001	28.13	0.797
C	In	0	4541	3.46	4.292	24	3.942	8	0.999	39.43	1.117
D	In	0	4876	3.29	4.293	25	3.961	11	1.004	31.59	0.895
average	In	0	···	3.40	4.249	···	3.946	···	1.000	35.30	1.000
E	In-Mn	214	4227	3.70	≈3.15	≈18	···	···	···	···	···
F	In-Mn	214	3087	4.66	3.330	33	3.148	16	0.798	18.84	0.534
G	In-Mn	214	2810	4.32	3.171	39	3.124	14	0.792	19.99	0.566
H	In-Mn	214	5295	3.71	3.240	22	3.214	35	0.815	18.47	0.523
I	In-Mn	325	4176	3.63	2.595	12	2.528	40	0.643	15.53	0.440
J	In-Mn	325	3977	3.81	2.686	26	2.622	24	0.664	12.69	0.360
K	In-Mn	396	3718	4.23	2.505	34	2.452	30	0.621	9.30	0.264
L	In-Cr	164	4671	3.73	3.614	76	3.350	21	0.849	22.83	0.647

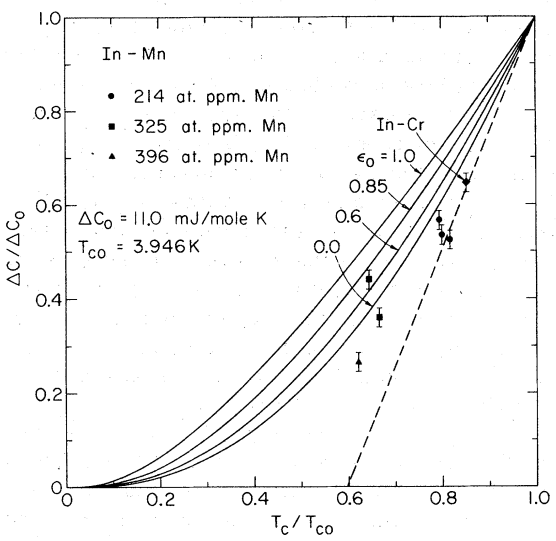

FIG. 9. Normalized discontinuity $\Delta c/\Delta c_0$ in the specific heat at the superconducting transition vs reduced transition temperature T_c/T_{c0}, where Δc_0 and T_{c0} are the values for the pure superconductor. These values are the averages of the results for the four films of pure indium. The solid curves are predictions based on the Shiba theory, and ϵ_0 is a parameter related to the strength of the interaction between the magnetic impurity and the conduction electrons of the superconductor. The allowed values of ϵ_0 range between 0 and 1. The dashed line represents the maximum initial depression of Δc predicted by Müller-Hartmann and Zittartz. The error bars represent the estimated uncertainty of our measurements.

termination of the mean. For the discontinuity in the specific heat of the pure superconductor, Δc_0, we obtained 11.0 mJ/K mol, with an uncertainty of less than 10% in the determination of the mean. The measurements of the transition temperature agree well with the results of other workers.[3,6] No one else has measured Δc for quench-condensed indium, so it is difficult to compare our results directly with any previous measurements. We do note that measurements on samples of bulk indium indicate a transition temperature of about 3.40 K and a discontinuity in the specific heat of

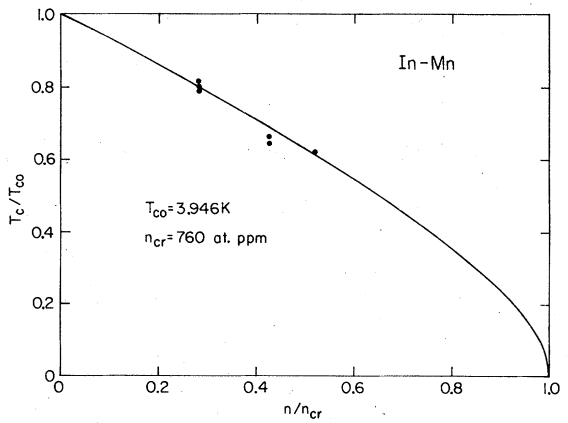

FIG. 10. Reduced transition temperature T_c/T_{c0} vs reduced impurity concentration n/n_{cr}, where T_{c0} is the transition temperature of the pure superconductor, and n_{cr} the critical concentration. The solid curve represents the prediction of Abrikosov and Gor'kov. The lower point at $n/n_{cr} \simeq 0.4$ corresponds to the higher of the two 325-at. ppm-Mn points in Fig. 9.

about 9.9 mJ/K mol.[40-42] Scaling this discontinuity to the transition temperature of quench-condensed indium (i.e., multiplying by 3.946/3.40, the ratio of the transition temperatures) gives 11.4 mJ/K mol, which is in fairly good agreement with our measured value.

The surprising result of our measurements on the pure films was the large spread in the results for Δc. We estimated that our measurements of Δc should be uncertain by about 2%, and yet the results for the pure indium films showed a variation which was greater than that. The explanation would appear to involve differences in the amount of disorder present in the various samples, presumably due to variations in the preparation of the samples. Bergmann has shown that the transition temperature and the width of the energy gap of pure indium increase with the degree of disorder.[43] For a BCS superconductor,[44] Δc is proportional to the width of the energy gap, so Δc would also be expected to increase with the degree of disorder. Bergmann used as his measure of the degree of disorder the ratio of the residual resistivity of his indium samples to the temperature-dependent resistivity at 273 K. If one plots our results of Δc against the residual resistivity of the films (Fig. 11), one finds that there does indeed appear to be a simple relationship of the expected type. If we use Bergmann's results to make an estimate of the dependence of Δc on the residual resistivity (assuming that Δc scales directly with the width of the energy gap), we find that the best-fit line through our data has a slope about ten times that which we would predict. However, the comparison is difficult because we could not measure the room-temperature resistivities of our samples. Furthermore, Bergmann's data have sufficient scatter to make the prediction for the slope uncertain by at least a factor of 2.

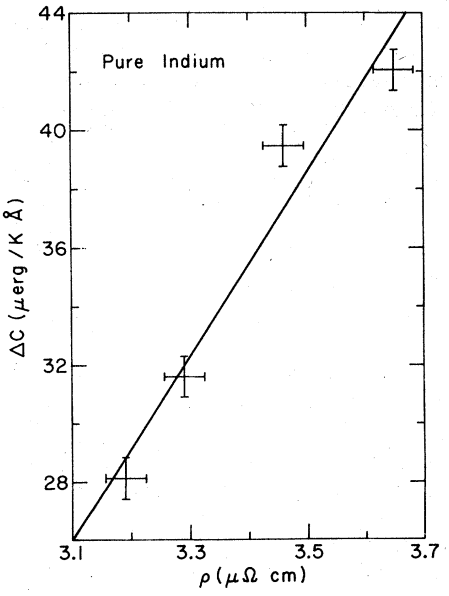

FIG. 11. Discontinuity in the specific heat, Δc, plotted against the residual resistivity ρ of the pure indium samples. The line represents the best linear fit to the data. The error bars represent the estimated uncertainty of our measurements.

B. Indium-manganese and indium-chromium alloys

The normalized discontinuities in the specific heat for the alloy films are plotted against the normalized transition temperature in Fig. 9. The depression of Δc with the introduction of magnetic impurities is so great that our results give lower values for $\Delta c/\Delta c_0$ than are predicted by the Shiba theory. This is also true for the results found previously for Zn-Mn,[27] Zn-Cr,[28] Mo-Fe,[29] and some cerium alloys.[45-49]

The Shiba theory is usually applied by taking into account only s-wave scattering of the d electrons from the impurity atoms. It has been noted that by removing this assumption it is possible to better explain the sharp depression of T_c with impurity concentration.[50,51] It is not likely that this sort of extension would resolve the disagreement found here, however. The maximum depression of $\Delta c/\Delta c_0$ relative to T_c/T_{c0} is obtained for $\epsilon_0 = 0$ in the Shiba theory. If we include the higher orbital angular momentum terms with $\epsilon_2 = \epsilon_1 = \epsilon_0 = 0$, where $\epsilon_1\Delta$ and $\epsilon_2\Delta$ are the energies of the states arising from the p- and d-wave scattering, Δc is more sharply depressed with impurity concentration. However, T_c is similarly affected, so that one obtains exactly the same dependence of $\Delta c/\Delta c_0$ on T_c/T_{c0} as when the higher orbital angular momentum terms are ignored.

Nor can the discrepancy between our data and the Shiba theory be resolved by supposing that in the alloy films Δc is a function of disorder, as for the pure films. We find no correlation between Δc and the resistivity of the alloy films; apparently the effects of the magnetic impurities are so great as to mask the effects of disorder. Furthermore, the residual resistivities of the alloy films are almost all higher than even the highest value recorded for the pure films, so any attempt to adjust our results for Δc on the basis of the residual resistivity of the sample would only amplify the disagreement between our data and the Shiba theory.

The more fully quantum-mechanical approach of MHZ may, however, lead to better agreement between our data and the theoretical predictions, as

indicated by the dashed line in Fig. 9, which represents the maximum initial slope according to MHZ.[20]

The data for run I indicate an anomalously high result for Δc. For completeness we have shown this result (the higher of the two 325-at. ppm-Mn points) along with the results for the other samples in Fig. 9. However, we consider the results for run I to be suspect, especially because, based on the impurity concentration, the transition temperature for that sample was anomalously low. (The transition temperature for run I is shown as the lower of the two points at $n/n_{cr} \simeq 0.4$ in Fig. 10.)

VII. CONCLUSIONS

Despite good agreement of thermal-conductivity measurements[4,5] with the Shiba theory, we find there is significant disagreement between the predictions of the theory and our measured discontinuity in the normalized specific heat $\Delta c/\Delta c_0$. Nonetheless, the Shiba theory represents an advance over the AG theory in that the Shiba curve for $\epsilon_0 = 0$ fits our results better than the AG curve ($\epsilon_0 = 1$). The work of MHZ indicates that a more fully quantum-mechanical approach to the impurity spin may remove some of the remaining disagreement between the theory and the experimental results. In any case, prior to these measurements the only systems which had shown such sharp depressions of $\Delta c/\Delta c_0$ involved transition-metal superconductors. By the present work it has been shown that this sharp depression is not limited to such systems.

Another important, although at present tentative, conclusion is that for pure indium films Δc is strongly dependent on the degree of disorder of the film. This is an effect which should be studied more systematically. Previous measurements on the width of the energy gap and the transition temperature of indium show that the ratio of these two quantities increases with increasing disorder.[43] Strong-coupling superconductors display large values for this ratio, so these measurements indicate that increased disorder leads to strong coupling in indium.[52] This suggests that measurements on indium of Δc as a function of disorder could be used to study further the effects of strong coupling on Δc. It would also be useful to carry out similar measurements on tin, where data are available which relate the transition temperature and energy gap to the degree of disorder.[43]

ACKNOWLEDGMENTS

We are grateful to John X. Przybysz and Thomas R. Lemberger for making some of the alloy ingots. We also thank the DOE for their support under Grant No. EY-76-C-02-1198.

---

*Based in part on the Ph.D. thesis of B. C. Gibson, University of Illinois, 1978 (unpublished).
†Present address: Space and Communications Group, Hughes Aircraft Co., P. O. Box 92919, Los Angeles, Calif. 90009.
‡Present address: TRIAD Computing Systems, Ltd., London, England.

[1]D. M. Ginsberg, Phys. Rev. B 15, 1315 (1977).
[2]B. J. Mrstik and D. M. Ginsberg, Phys. Rev. B 7, 4844 (1973).
[3]A. W. Bjerkaas, D. M. Ginsberg, and B. J. Mrstik, Phys. Rev. B 5, 854 (1972).
[4]J. X. Przybysz and D. M. Ginsberg, Phys. Rev. B 14, 1039 (1976).
[5]J. X. Przybysz and D. M. Ginsberg, Phys. Rev. B 15, 2835 (1977).
[6]T. R. Lemberger and D. M. Ginsberg, Phys. Rev. B 18, 6105 (1978).
[7]K. Maki, in *Superconductivity*, edited by R. D. Parks (Dekker, New York, 1969), Vol. II, p. 1035.
[8]W. Buckel and R. Hilsch, Z. Phys. 128, 324 (1950).
[9]B. T. Matthias, H. Suhl, and E. Corenzwit, Phys. Rev. Lett. 1, 92 (1958).
[10]P. W. Anderson, J. Phys. Chem. Solids 11, 26 (1959).
[11]A. A. Abrikosov and L. P. Gor'kov, Zh. Eksp. Teor. Fiz. 39, 1781 (1960) [Sov. Phys. JETP 12, 1243 (1961)].
[12]S. Skalski, O. Betbeder-Matibet, and P. R. Weiss, Phys. Rev. 136, A1500 (1964).
[13]M. B. Maple, in *Magnetism*, edited by H. Suhl (Academic, New York, 1973), Vol. V, p. 289.
[14]M. A. Woolf and F. Reif, Phys. Rev. 137, A557 (1965).
[15]G. J. Dick and F. Reif, Phys. Rev. 181, 774 (1969).
[16]H. Shiba, Prog. Theor. Phys. 40, 435 (1968).
[17]A. I. Rusinov, Zh. Eksp. Teor. Fiz. 56, 2047 (1969) [Sov. Phys. JETP 29, 1101 (1969)].
[18]A. N. Chaba and A. D. S. Nagi, Can. J. Phys. 50, 1736 (1972).
[19]E. Müller-Hartmann, in *Magnetism*, edited by H. Suhl (Academic, New York, 1973), Vol. V, p. 353.
[20]E. Müller-Hartmann and J. Zittartz, Z. Phys. 256, 366 (1972).
[21]E. Müller-Hartmann and J. Zittartz, Phys. Rev. Lett. 26, 428 (1971).
[22]B. Schuh and E. Müller-Hartmann, Z. Phys. B29, 39 (1978).
[23]R. D. Parks, in *Superconductivity*, edited by P. R. Wallace (Gordon and Breach, New York, 1969), Vol. II, p. 625.
[24]S. Takayanagi and T. Sugawara, J. Phys. Soc. Jpn. 38, 718 (1975).
[25]D. L. Martin, Proc. Phys. Soc. London 78, 1489 (1961).
[26]F. W. Smith, J. Low Temp. Phys. 6, 435 (1972).
[27]F. W. Smith, J. Low Temp. Phys. 5, 683 (1971).
[28]R. Vaccarone, A. Morozzo della Rocca, A. Pilot, F. Vivaldi, and C. Rizzuto, Solid State Commun. 12, 885 (1973).
[29]S. Takayanagi, M. Takano, Y. Kimura, and T. Sugawara, J. Low Temp. Phys. 16, 519 (1974).

[30]W. Opitz, Z. Phys. 141, 263 (1955).
[31]G. Boato, M. Bugo, and C. Rizzuto, Nuovo Cimento B 45, 226 (1966).
[32]B. C. Gibson, Ph.D. thesis, University of Illinois, Urbana, 1978 (unpublished).
[33]J. M. Mochel (private communication).
[34]G. D. Zally and J. M. Mochel, Phys. Rev. B 6, 4142 (1972).
[35]Varian Associates, Vacuum Division, Palo Alto, Calif. 94302.
[36]P. Sullivan and G. Seidel, Ann. Acad. Sci. Fenn. Ser. A 210, 58 (1966).
[37]P. Sullivan and G. Seidel, Phys. Rev. 173, 679 (1968).
[38]E. L. Griffin, Ph.D. thesis, University of Illinois, 1975 (unpublished).
[39]S. Tolansky, *Multiple-Beam Interferometry of Surfaces and Films* (Oxford University, New York, 1948).
[40]J. R. Clement and E. H. Quinnell, Phys. Rev. 92, 258 (1953).
[41]C. A. Bryant and P. H. Keesom, Phys. Rev. 123, 491 (1961).
[42]H. R. O'Neal and N. E. Phillips, Phys. Rev. 137, A748 (1965).
[43]G. Bergmann, Z. Phys. 228, 25 (1969).
[44]J. Bardeen, L. N. Cooper, and J. R. Schrieffer, Phys. Rev. 108, 1175 (1957).
[45]C. A. Luengo, M. B. Maple, and W. A. Fertig, Solid State Commun. 11, 1445 (1972).
[46]H. Armbrüster, H. von Löhneysen, G. Riblet, and F. Steglich, Solid State Commun. 14, 55 (1974).
[47]F. Steglich and H. Armbrüster, Solid State Commun. 14, 903 (1974).
[48]F. Steglich, Z. Phys. B23, 331 (1976).
[49]T. Aoi and Y. Masuda, J. Phys. Soc. Jpn. 34, 271 (1973).
[50]H. Shiba, Prog. Theor. Phys. 50, 50 (1973).
[51]D. M. Ginsberg, Phys. Rev. B 10, 4044 (1974).
[52]G. Bergmann, Phys. Rep. 27, 159 (1976).